

1 **Field-scale assessment of direct and indirect effects of soil texture on organic matter**
2 **mineralization during a dry summer**

3 **Authors:**

4 Haichao Li ^{a, b*}, Astrid François ^{a, c}, Xiaolin Wang ^d, Shengmin Zhang ^e, Orly Mendoza ^{a, f, g},
5 Stefaan De Neve ^a, Kevin Dewitte ^h, Steven Sleutel ^a

6 **Affiliations and addresses:**

7 ^a Research Group of Soil Fertility and Nutrient Management, Department of Environment, Ghent
8 University, Coupure Links 653, 9000 Ghent, Belgium

9 ^b Department of Soil and Environment, Swedish University of Agricultural Sciences, Lennart
10 Hjelms väg 9, 750 07 Uppsala, Sweden

11 ^c Isotope Bioscience Laboratory, Department of Green Chemistry and Technology, Ghent
12 University, Coupure Links 653, 9000 Ghent, Belgium

13 ^d Department of Sustainable Environment and Construction, Mälardalen University, 722 23
14 Västerås, Sweden

15 ^e SLU Swedish Species Information Center, Swedish University of Agricultural Sciences, 75007
16 Uppsala, Sweden

17 ^f Institute of Earth Surface Dynamics, University of Lausanne, 1015 Lausanne, Switzerland

18 ^g School of Architecture, Civil and Environmental Engineering EPFL, 1015 Lausanne, Switzerland

19 ^h Department of Plants and Crops, Ghent University, Coupure Links 653, 9000 Ghent, Belgium

20 *** Corresponding Author:** Email: haichao.li91@gmail.com

21

22 **Abstract**

23 Soil texture plays a crucial role in organic matter (OM) mineralization through both direct
24 interactions with minerals and indirect effects on soil moisture. Separating these effects could
25 enhance the modelling of soil organic carbon (SOC) dynamics under climate change scenarios.
26 However, the attempts have been limited small-scale experiments. Here, we studied the effects of
27 soil texture on added OM mineralization in loamy sand, loam and silt loam soils in nine agricultural
28 fields in Flanders, Belgium. Soil moisture, temperature, groundwater table depth and the
29 mineralization of ^{13}C -labeled ryegrass were monitored in buried mesocosms for approximately
30 three months during a dry summer. Ryegrass-C mineralization was lowest in the loamy sand
31 ($39\pm 7\%$) followed by silt loam ($48\pm 7\%$) and loam ($63\pm 5\%$) soils, challenging the current clay%-
32 based moderation of C-mineralization rates in soil models. Soil temperature was not influenced by
33 soil texture, whereas soil moisture was indeed dependent on soil texture. It appears that capillarity
34 sustained upward water supply from groundwater to the topsoil in loam and silt loam soils but not
35 in loamy sand soil, although this difference in capillary rise could not fully explain the higher
36 moisture content in loam than that in silt loam soils. Additionally, soil texture only impacted
37 remnant added ryegrass pieces ($>500\ \mu\text{m}$) but not the finer ryegrass-derived SOC ($<500\ \mu\text{m}$),
38 which might point at the important indirect control of texture on OM mineralization during
39 prolonged summer drought. However, these effects are only manifested during drought when no
40 other factors (e.g., groundwater depth or subsurface water flows) exert an overriding impact on the
41 soil water balance. Overall, our findings highlight the need to properly incorporate the indirect
42 effects of soil texture on OM mineralization into soil carbon models to accurately predict soil C
43 stocks under future climate change scenarios.

44 **Keywords:** Capillary rise; Groundwater; Soil moisture; Soil organic carbon; Stable carbon isotope

45 **1. Introduction**

46 Together with moisture and temperature, soil texture is a key factor controlling soil organic carbon
47 (SOC) content (Burke et al., 1989; Blanco-Moure et al., 2016). Soil texture controls SOC dynamics
48 directly by a myriad of direct interactions with organic matter (OM). The high specific surface
49 area and net negative charge of most clay minerals facilitate the binding of OM, and this retards
50 OM mineralization (Krull et al., 2003). For instance, Plante et al. (2006) found that biochemically
51 protected C strongly correlated with clay content while soil texture had little impact on the content
52 of particulate OM. In fact, the stabilizing action of soil minerals on SOC has been recognized for
53 over two centuries (Feller and Chenu, 2012) and has been integrated into SOC models for decades
54 (Parton et al., 1987; Jenkinson et al., 1990; Barré et al., 2017). Soil aggregation is also enhanced
55 in finer textured soil, and OM within aggregates can be “protected” from mineralization (Beare et
56 al., 1994; Krull et al., 2003). Numerous studies concluded that soil respiration decreases with finer
57 soil texture because of these physicochemical OM protection mechanisms (Van Veen et al., 1985;
58 Hassink, 1992; Wang et al., 2003; Muller and Hoper, 2004). These “direct” effects of soil texture
59 explain the generally increasing SOC levels with higher clay and silt content under similar climatic
60 conditions (Burke et al., 1989; Blanco-Moure et al., 2016).

61 Apart from these well-studied “direct” textural effects, there is much less information on how
62 strongly soil texture influences OM mineralization indirectly through its control on the soil
63 moisture balance. With more silt and clay, the pore size distribution shifts to smaller pores and
64 water holding capacity increases, resulting in contrasting soil moisture content in differently
65 textured soils for a given water input (Geroy et al., 2011). Thomsen et al. (1999) reported that
66 microbial activity was higher in finer-textured soils than that in coarser ones specifically because
67 more water was retained. When adding equal amounts of water to three distinctly textured soils

68 and allowing soils to dry out, Li et al. (2020) concluded that C mineralization was strongly
69 indirectly modulated by soil texture via its impact on soil moisture, with less evaporative losses
70 from finer- than from coarser-textured soil. However, these studies were laboratory based with
71 strict control of soil moisture and temperature. In the more complex field reality, soil
72 microorganisms are subjected to fluctuations in soil temperature and moisture, and such fluctuation
73 is well known to strongly impact soil heterotrophic activity. Under field conditions, Dilustro et al.
74 (2005) found that soil CO₂ emission was indirectly controlled by soil texture through moisture
75 during a dry season in forest soils. Zhang et al. (2015) found that desert dune soil physical
76 properties, such as soil texture and field capacity, exerted strong influences on soil respiration
77 through affecting its relation with soil water content. In a soil texture manipulation field
78 experiment with all other factors kept equal, Li et al., (2022) demonstrated that during dry summer
79 months OM mineralization was strongly controlled by soil texture, and in particular through its
80 impact on soil moisture. However, none of these few studies on this topic allowed to unequivocally
81 discern the direct and indirect textural controls on mineralization of SOC or newly added OM.
82 Moreover, only limited numbers of sites were included and no larger-scale field assessment has
83 been conducted to investigate indirect vs. direct controls of soil texture on OM mineralization.

84 Under field conditions, the topsoil moisture can be influenced by shallow groundwater through
85 capillary rise (Zipper et al., 2015; Smith et al., 2017). In low-flat landscapes, such as in The
86 Netherlands and Northern Belgium, many agricultural lands have shallow groundwater tables
87 (GWTs) (<2.5 m). In fact, shallow groundwater accounts for up to 32% of global land area and in
88 dry summers it might be critical for topsoil moisture supply through capillary rise (Fan et al., 2013).
89 Next to groundwater depth and topsoil moisture level, soil texture controls the flux and extent of
90 this upward moisture supply with maximal capillary rise height of only 0.2-1.3 m in sand and >3

91 m in silt (Liu et al., 2014; Zipper et al., 2015; Salim, 2016). However, it is still unclear whether
92 this indirect texture-mediated effect on soil moisture profiles is crucial for OM mineralization in
93 the topsoil during a dry summer.

94 The objective of this study was to systematically investigate the direct (through physicochemical
95 stabilization) and indirect (through textural controls on soil moisture) effects of soil texture on OM
96 mineralization in croplands during a dry summer period. To this end, we followed mineralization
97 of ¹³C-labeled ryegrass at eighteen plots distributed over nine agricultural fields covering three soil
98 textures, i.e. loamy sand, loam and silt loam, with detailed follow-up of soil moisture and
99 temperature. Extra control treatments with a single reference soil at all plots were included to
100 assess the indirect textural control on OM (i.e. ryegrass) mineralization. We expected that during
101 dry summer months ryegrass-C mineralization would proceed overall slower in the “reference”
102 soil when buried in loamy sand textured fields as these soils dry out faster compared to finer
103 textured loam and silt loam fields. We also expected that shallow groundwater would maintain
104 topsoil water supply in silt loam and loam soil through capillary rise, but not in loamy sand soils,
105 which again would hinder OM mineralization in the loamy sand fields. In buried mesocosms
106 containing the original soils both indirect and direct soil textural effects on OM mineralization
107 would counteract: lesser physicochemical protection of OM in coarser-textured soil but at the same
108 time a stronger drying out of topsoil compared to in finer textured fields. How the interaction
109 between these phenomena would impact OM mineralization is difficult to predict as it depends on
110 how limiting topsoil moisture content becomes. The direct stabilizing effect of finer texture would
111 predominantly control OM mineralization if sufficient moisture were available in all soils. In
112 contrast, OM mineralization would proceed in finer-textured soils under drought, while it would
113 become strongly moisture-limited in coarse textured soil.

114 **2. Materials and Methods**

115 *2.1. Overall experimental design*

116 An extensive assessment of OM mineralization in cropland soils as a function of soil texture was
117 set out *in situ* with buried soil mesocosms in which mineralization of a ¹³C isotope-labeled ryegrass
118 substrate (see 2.3) was monitored. These buried mesocosms were distributed over nine agricultural
119 fields in the Province of East Flanders, Belgium, covering three soil textures, i.e., loamy sand,
120 loam and silt loam. In each field, we laid out two plots, thus totaling eighteen plots. In each plot,
121 the buried native and reference soil mesocosms (see 2.4) were taken out after about three months.
122 We assumed that in the soil mesocosms filled with the native soil, soil texture exerts both a direct
123 control on OM mineralization, via its steering of OM-mineral phase interactions, as well as an
124 indirect control via mediation of the soil moisture content in the field. In order to study the indirect
125 effect of soil texture on OM mineralization via its regulation of soil moisture, a parallel set of
126 reference soil mesocosms (with a loamy sand soil from plot 1-1, see Table 1) was included at each
127 plot (Fig. 1). By using the same soil in the reference mesocosms, any direct textural effect on OM
128 mineralization was eliminated, allowing to study indirect soil moisture effects on OM
129 mineralization in isolation.

130 **Table 1** Basic properties of the studied soils.

Plot No.	Texture (USDA)	Sand (%)	Silt (%)	Clay (%)	SOC (g kg ⁻¹)	$\delta^{13}\text{C}$ (‰)	C/N ratio (-)	pH-KCl (-)	Elevation (m a.s.l)*
1-1	loamy sand	84.6	12.7	2.8	8.6	-25.2	8.9	6.6	24.0
1-2	loamy sand	79.7	17.3	3.0	9.0	-25.7	8.6	5.1	18.8
2-1	sandy loam	77.9	11.2	10.9	9.0	-24.9	8.2	5.0	27.6
2-2	loamy sand	85.1	10.2	4.7	13.8	-26.1	9.9	6.2	21.1
3-1	loamy sand	80.9	15.3	3.8	8.8	-27.2	8.2	5.5	38.9
3-2	loamy sand	83.9	12.7	3.4	7.5	-26.7	7.9	5.3	36.1
4-1	loam	49.0	42.4	8.6	15.6	-27.0	9.6	5.9	29.2
4-2	loam	43.9	47.3	8.8	16.2	-26.9	9.5	6.0	25.0
5-1	loam	49.0	44.0	7.0	9.2	-26.3	8.4	5.4	30.7
5-2	loam	44.0	48.9	7.1	10.2	-25.9	9.3	5.9	25.2
6-1	sandy loam	50.2	47.3	2.5	15.9	-26.6	10.7	6.4	25.0
6-2	loam	48.6	43.7	7.7	11.1	-27.4	8.7	6.2	21.1
7-1	silt loam	14.1	74.2	11.7	14.7	-26.8	9.5	6.6	51.2
7-2	silt loam	15.0	73.2	11.8	12.7	-26.8	8.6	6.5	45.2
8-1	silt loam	36.2	52.8	11.0	11.5	-25.8	9.9	6.7	58.9
8-2	silt loam	12.9	76.3	10.8	15.4	-27.3	9.0	6.0	50.3
9-1	silt loam	22.8	65.8	11.4	13.6	-27.1	9.2	5.9	60.0
9-2	silt loam	15.9	72.6	11.5	16.4	-27.2	9.3	5.3	54.7

131 * m a.s.l: Meters above sea level

132

133 *2.2. Field plots*

134 The study area has a maritime climate, with mean temperature and annual precipitation during
 135 1992-2013 of 10.7 °C and 872 mm, respectively. Daily air temperature and precipitation data were
 136 collected by a weather station at the Ghent University experimental farm in Bottelare, Belgium.

137 The annual precipitation in 2020 was 872 mm, identical to the 1992-2013 average, while
 138 precipitation was only 196 mm within the experimental period (from May 26th to September 1st),
 139 i.e. only 65% of the mean precipitation in 1992-2013 for the same period (Fig. 2a). Nine cropland
 140 fields were preselected based on the digital Belgian soil map, which provides an indication of soil

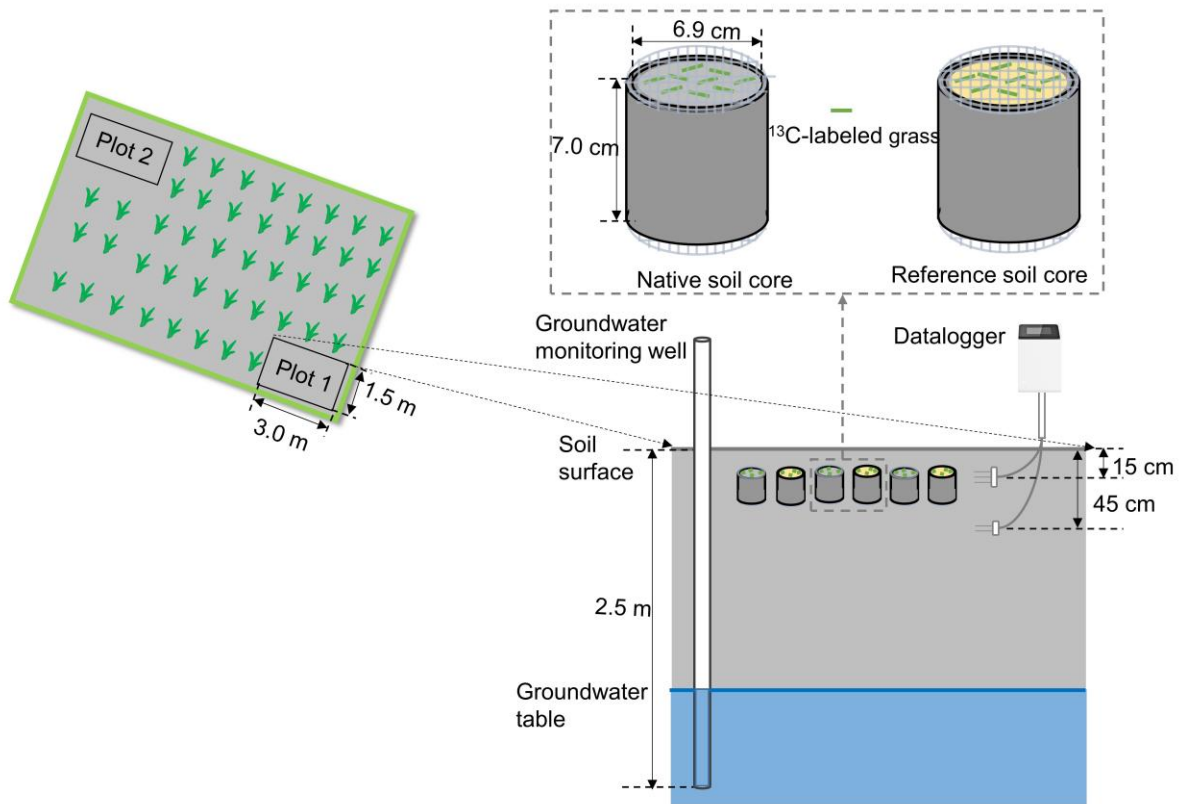
141 texture and soil drainage classes. We specifically chose three field replicates per soil textural class
142 (loamy sand, loam and silt loam) with comparable expected GWTs. Two plots were chosen in each
143 field, totalling six plots per soil textural class (Table 1). At each of these eighteen locations, 1.5 m
144 × 3.0 m plots were set out in which the soil mesocosms were incorporated. These data were
145 considered representative for all nine cropland fields situated within 20 km distance. The
146 characteristics (soil texture, soil pH, soil C and N content, and soil $\delta^{13}\text{C}$) of the studied soils are
147 shown in Table 1. Soil texture of the field replicates per intended textural class was alike. One
148 exception was plot 2-1, with a somewhat deviating sandy loam texture (USDA classification),
149 although in absolute terms its sand and silt contents were well comparable to the other loamy sand
150 replicate fields. Therefore, we denoted plots 1-1 to 3-2 as loamy sand soils, plots 4-1 to 6-2 as
151 loam soils and plots 7-1 to 9-2 as silt loam soils (Table 1). All soils had a comparable C/N ratio
152 (~9) and pH (~6), while the mean native SOC was higher in the silt loam soils ($14.1 \pm 0.7 \text{ g kg}^{-1}$)
153 than in the loamy sand soils ($9.4 \pm 0.9 \text{ g kg}^{-1}$) ($P < 0.05$). Soil water retention curves for the eighteen
154 undisturbed field soils at 15 cm and 45 cm depth were determined by measuring moisture content
155 at -1, -3, -7, -10 kPa using a sandbox (Eijkelkamp Agrisearch Equipment, The Netherlands) and
156 at -33, -100, and -1500 kPa using a pressure membrane (Soil Moisture Equipment, USA) (Fig.
157 S1 and Fig. S2). The water retention curves were fitted with the RECT programme (Van
158 Genuchten et al., 1991) using van Genuchten equation (Van Genuchten, 1980).

159

160

161

162



164

165 **Fig. 1** Schematic of two plots in one out of nine included cropland fields (left) and side view of a
 166 single plot (lower right) with buried mesocosms containing native and reference soils in which
 167 ^{13}C -labeled ryegrass was mixed. The top and bottom of the mesocosm PVC tubes were covered
 168 with a nylon mesh to allow contact and free equilibration of moisture between the soil in the tube
 169 and the surrounding field soil (upper right). Volumetric soil moisture content and temperature were
 170 measured at 15 cm depth using a TEROS 12 sensor and soil moisture once more at 45 cm depth
 171 using a TEROS 10 sensor. A 2.5 m-deep groundwater monitoring well was established at each
 172 plot.

173

174 2.3. Production of ^{13}C labeled ryegrass

175 Isotopic (^{13}C) labeled ryegrass (*Lolium perenne* L.) was produced at the Ghent University
 176 experimental farm (Bottelare, Belgium). Prior to ^{13}C -labeling, ryegrass was cut to 2 cm above-
 177 ground from nine 0.8×0.8 m plots in a permanent ryegrass field. The ryegrass was then weekly

178 pulse-labeled with ^{13}C - CO_2 between August 2nd and September 27th, 2019, using custom-made 0.8
179 $\times 0.8 \times 0.3$ m Plexiglass labeling chambers. The $^{13}\text{CO}_2$ concentration in the labeling chamber was
180 brought to about 500 ppmv by injecting 0.2 mol L^{-1} HCl solution into a recipient containing
181 $\text{NaH}^{13}\text{CO}_3$ (98 Atom%) solution in each labeling event. The generated ^{13}C - CO_2 was circulated by
182 battery-powered fans in the sealed chambers and allowed to be evenly taken up by the ryegrass.
183 Chambers were always installed around 9 a.m. and were kept closed for 24 hours, allowing re-
184 uptake of the nighttime respired ^{13}C - CO_2 by the ryegrass in the next morning. To increase biomass
185 productivity, KNO_3 was applied at a rate of 60 kg N ha^{-1} . After eight weeks, the ryegrass above-
186 ground parts were manually harvested (to 2 cm above the surface) and then dried at 60 °C for 72
187 hours. The ^{13}C -labeled ryegrass had a C content of $39.6 \pm 0.2\%$, N content of $3.1 \pm 0.0\%$ and $\delta^{13}\text{C}$ of
188 $+53.7 \pm 2.7\text{‰}$. Young and matured ryegrass plant parts differed in $\delta^{13}\text{C}$ by only 3.8‰, indicating
189 homogeneous labeling.

190 *2.4. Preparation and sampling of soil mesocosms*

191 Soils were collected from the eighteen different locations on the verge of each plot at the 10-20
192 cm depth layer, which is known to represent the top agricultural soils in the Flanders region. In the
193 laboratory, these field moist soils were passed through a 5 mm sieve and larger plant debris and
194 gravel left on the sieve were removed. The ^{13}C -enriched ryegrass was cut into pieces of
195 approximately 2–4 cm length and mixed with soil at a dose of 2.5 g dry matter kg^{-1} soil, equivalent
196 to 1.0 g C kg^{-1} soil. To eliminate differences in N availability among the used soils, KNO_3 was
197 added at a dose of 24.7 mg kg^{-1} (equivalent to about 100 kg N ha^{-1}). After mixing thoroughly,
198 soils were repacked at a bulk density of 1.35 g cm^{-3} into 7.0 cm high and 6.9 cm diameter PVC
199 tubes. The top and bottom of the PVC tube were covered with a nylon mesh (0.5 mm opening), to
200 allow free equilibration of moisture between the soil in the tube and the surrounding field soil (Fig.

201 1). Next to soil from the original field (here termed “native soils”), a parallel set of reference soil
202 (loamy sand soil from plot 1-1 in Table 1) mesocosms was also included at each experimental plot
203 to specifically investigate the indirect textural control on OM mineralization through its impact on
204 soil moisture.

205 All soil cores were incorporated at 15 cm depth into plots measuring 1.5 m by 3.0 m at the 18
206 field locations (Fig. 1). These plots were established close to the edges of the selected croplands
207 excluding tractor traffic and without growing crop (Fig. 1). The soil mesocosms were incorporated
208 in the plots on May 26th, 2020 and taken out on September 1st, 2020. In total, 108 soil mesocosms
209 (3 mesocosm replicates × 6 field replicates per texture × 3 soil textures × 2 treatments (native soil
210 and reference soil) were prepared. During the short period between preparation and incorporation,
211 soil cores were stored at 4 °C to minimize microbial activity.

212 *2.5. Estimation of ryegrass-C mineralization*

213 After recollecting mesocosms from the plots, the field-moist soil cores were gently broken apart
214 by hand and they were passed through a 4-mm sieve. Large pieces of roots, plant debris and small
215 stones were taken out manually. We distinguished between remnant undecomposed ryegrass-C
216 and ryegrass-derived SOC by sieving soils at 500 µm, and both fractions were assumed to
217 correspond to ryegrass-C left in the >500 µm and <500 µm soil fraction, respectively. To separate
218 these soil fractions, half of the total field moist soil (equivalent to ~175 g dry soil) was transferred
219 into a 1 L glass Erlenmeyer, dispersed by adding 350 ml of 5 g L⁻¹ sodium metaphosphate and by
220 shaking the suspensions for 1 h. After shaking, the mixtures were poured onto a 500 µm sieve and
221 the material remaining on the sieve, viz. undecomposed ryegrass, coarse particulate soil OM and
222 sand was rinsed gently with deionized water. The >500 µm fraction and suspension with soil <500
223 µm were transferred into aluminum cups and dried at 60 °C for 72 hours. Finally, these dried

224 samples were ball-milled and analyzed for their C % and $\delta^{13}\text{C}$ using an elemental analyzer-isotope
225 ratio mass spectrometer (PDZ Europa ANCA-GSL, Sercon, Cheshire, UK).

226 The ryegrass-C fraction of the total C in the $>500\ \mu\text{m}$ and $<500\ \mu\text{m}$ soil fraction ($f_{\text{ryegrass-C}}$) was
227 calculated with a simple isotope mixing model, following Balesdent and Mariotti (1996):

$$228 \quad f_{\text{ryegrass-C}} = \frac{\delta^{13}\text{C}_{\text{sample}} - \delta^{13}\text{C}_{\text{control}}}{\delta^{13}\text{C}_{\text{mixed}} - \delta^{13}\text{C}_{\text{control}}}, \quad (1)$$

229 where $\delta^{13}\text{C}_{\text{sample}}$, $\delta^{13}\text{C}_{\text{control}}$ and $\delta^{13}\text{C}_{\text{mixed}}$ are the $\delta^{13}\text{C}$ value of a given $>500\ \mu\text{m}$ (or $<500\ \mu\text{m}$)
230 sample, the $>500\ \mu\text{m}$ fraction (or $<500\ \mu\text{m}$) without ryegrass added and the initial $>500\ \mu\text{m}$ (or
231 $<500\ \mu\text{m}$) fraction with ryegrass mixed at onset of the experiment, respectively. $\delta^{13}\text{C}_{\text{control}}$ varied
232 between -27‰ and -24‰ (Table 1). $\delta^{13}\text{C}_{\text{mixed}}$ of $>500\ \mu\text{m}$ fractions and $\delta^{13}\text{C}_{\text{mixed}}$ of $<500\ \mu\text{m}$
233 fractions varied between -5‰ to $+12\text{‰}$, and between -23‰ to -17‰ , respectively, depending on
234 the corresponding soil OM fraction mass and native SOC content. Ryegrass-C mineralization was
235 calculated using the following equation:

$$236 \quad \text{Ryegrass-C mineralization (\%)} = 100 - f_{\text{ryegrass-C}>500\ \mu\text{m}} - f_{\text{ryegrass-C}<500\ \mu\text{m}}, \quad (2)$$

237 where $f_{\text{ryegrass-C}>500\ \mu\text{m}}$ and $f_{\text{ryegrass-C}<500\ \mu\text{m}}$ are the percentage of remaining ryegrass $>500\ \mu\text{m}$ and
238 $<500\ \mu\text{m}$ of the added ryegrass, respectively.

239 *2.6 Soil moisture, temperature and groundwater table*

240 Dataloggers and TEROS 12 (soil moisture and temperature) and TEROS 10 (soil moisture) sensors
241 (METER Group, USA) were used to monitor volumetric moisture content (θ_v) and soil temperature
242 every 12 hours from March 2020 to September 2020. The sensors were calibrated individually in
243 the used soils prior to the start of the experiment. Briefly, each soil was air-dried and water was
244 carefully added to each soil to reach a θ_v of 0.02, 0.08, 0.15, 0.25, 0.35 and then the soil was gently

245 compacted at a bulk density of 1.40 g cm⁻³. Consequently, the linear functions between the
246 measured and the pre-set values were calculated. The moisture values from the field measurements
247 were calibrated based on the calibration formulas specific to each soil. The sensors were installed
248 horizontally at 15 cm and 45 cm depth in each plot (Fig. 1). The mean soil temperature was on
249 average 19.3 °C across all soils (Fig. 2b), and was statistically identical in all soils. As water-filled
250 pore space (WFPS) eliminates differences in bulk density and reflects balancing between moisture
251 availability and aeration status in soil microbiological processes (Scott et al., 1996; Franzluebbers,
252 1999; Poll et al., 2013), the measured θ_v was converted into WFPS with the following equation:

$$253 \text{ WFPS (\%)} = \frac{\theta_v}{\left(1 - \frac{\text{bulk density}}{\text{particle density}}\right)} \times 100, \quad (3)$$

254 assuming a particle density of 2.65 Mg m⁻³. A 2.5-m depth groundwater measuring well was
255 installed at the border of each plot and the GWT depth was measured manually using a GWT
256 measuring tape on regular a basis (Fig. 1).

257 2.7. Statistical analysis

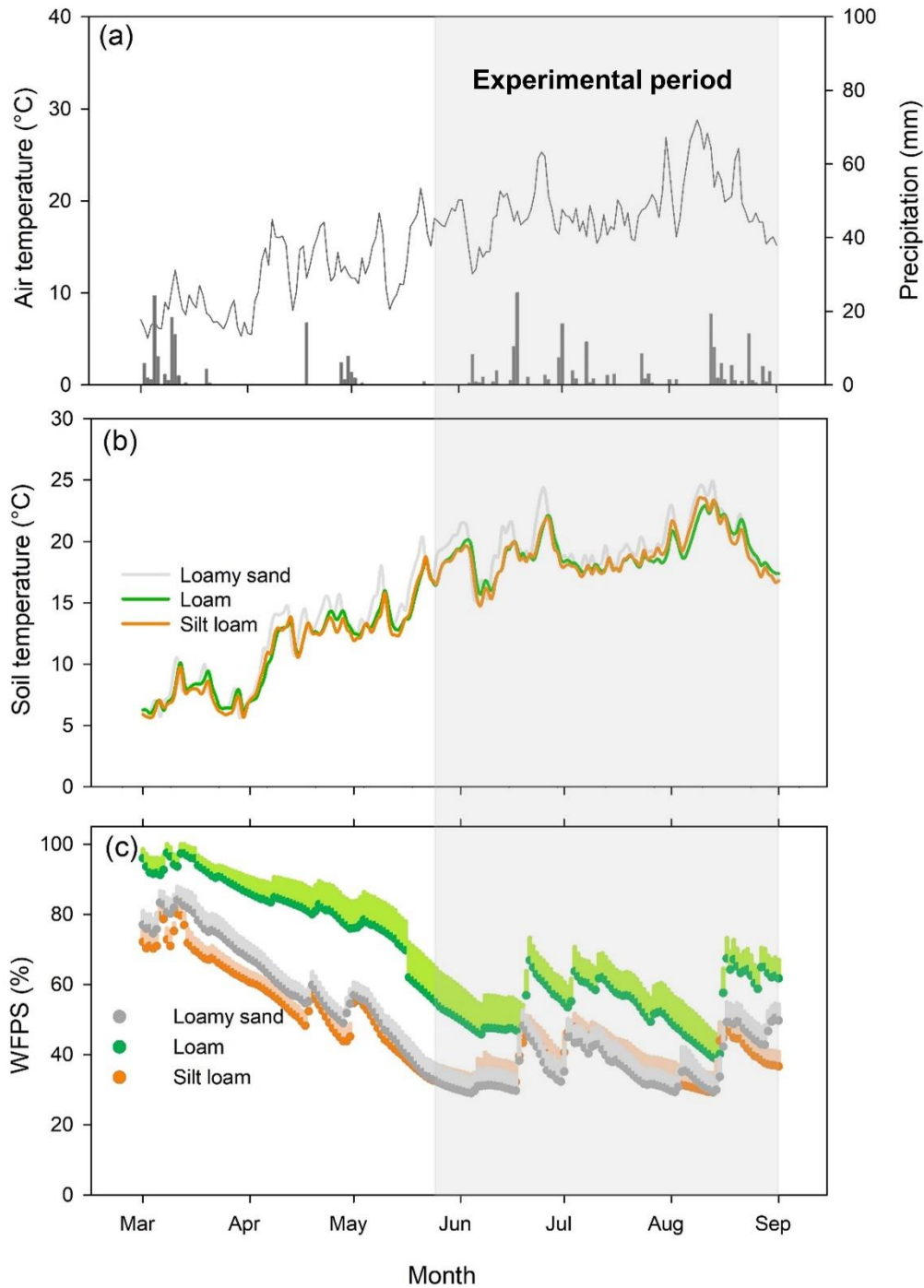
258 All analyses were performed in RStudio Version 1.3.1093. To test whether variation in initial SOC
259 content, soil pH, soil C/N ratio, ryegrass-C mineralization and the remaining undecomposed
260 ryegrass-C (>500 μm and <500 μm fractions) depended on soil texture, linear mixed effects models
261 (LMMs) were applied with ‘soil texture’ as fixed factor and ‘plot’ as random factor to account for
262 the hierarchical design of the experiment, using restricted maximum likelihood in the *lme* function
263 from the *nlme-package* (Zuur et al., 2009). Next, soil moisture content and soil temperature
264 measured over defined time periods among the three textural classes was compared using likewise
265 LMMs. To account for temporal autocorrelation of soil moisture content and soil temperature
266 (Koenig and Liebhold, 2016; Ruel and Ayres, 1999), the *corAR1(form=~Date)* variance structure

267 (Zuur et al., 2009), to test whether the values of soil moisture content and soil temperature
268 significantly differed between soil texture classes was incorporated. Multiple linear regression
269 analysis was employed to test the predictive power of %WFPS, soil temperature for ryegrass-C
270 mineralization for the different textures separately.

271 **3. Results**

272 *3.1. Soil moisture*

273 Soil moisture (%WFPS) followed a similar temporal pattern across the different textured soils,
274 with relatively high WFPS levels in the loamy sand and silt loam soils (~75%WFPS) and wetter
275 conditions (~90%WFPS) in the loam soils several months prior to onset of the experiment in
276 March 2020. Soil gradually dried at all plots thereafter until mid-June, shortly after the experiment
277 started. Subsequently, dry/wet cycles occurred in all soils in June-August 2020 (Fig. 2c). Using a
278 linear mixed model, we tested for statistical differences in the time-series data between the studied
279 textural classes during the experimental period. The average %WFPS followed the following order:
280 loam ($54 \pm 7\%$) > ($P < 0.05$) loamy sand ($37 \pm 5\%$) = silt loam ($37 \pm 5\%$).

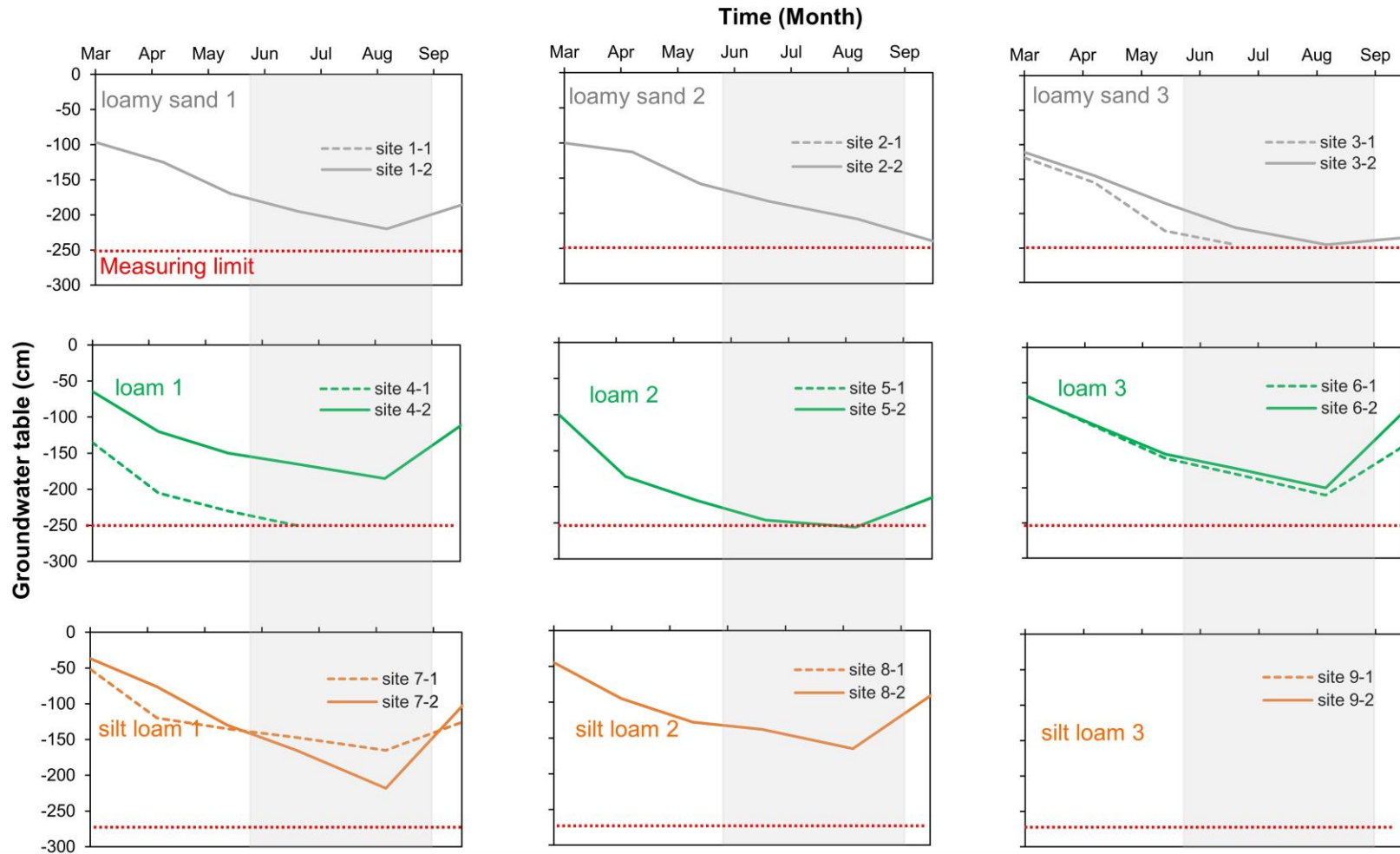


281

282 **Fig. 2** Daily average air temperature (line chart) and daily precipitation (bars) (a). Changes in soil
 283 temperature (°C) (b) and water-filled pore space percentage (%WFPS) (c) at 15 cm depth in the
 284 loamy sand, loam and silt loam soils. Error bars represent standard errors of soil moisture measured
 285 on all six field replicate plots per texture. Note: the error bars of soil temperature were not included
 286 in the figure as they were negligibly small. For %WFPS only upper error bars are shown.

287 3.2. *Groundwater Tables (GWTs)*

288 Throughout the experimental period, there were two, one, and three plots where GWTs reached
289 deeper levels than the 2.5 m monitoring well limit for the loamy sand, loam, and silt loam classes,
290 respectively (Fig. 3). GWTs were at the shallowest levels around March 2020 after which they
291 gradually lowered to minima by September 2020. Except for the plots where GWTs were deeper
292 than the monitoring limit, GWTs were all approximately 1.5-2.5 m deep during the experimental
293 period (Fig. 3).



294

295 **Fig. 3** Trends in groundwater table depth in the nine studied fields with two plots per field. The grey rectangle shade indicates the
 296 experimental period. For some of the plots no data was available as groundwater was below the measuring limit of the monitoring well
 297 (2.5 m: indicated by a red dashed line).

298 3.3. Ryegrass-C mineralization and undecomposed ryegrass

299 3.3.1 Ryegrass-C mineralization

300 As explained in 2.1, in each microplot ryegrass C mineralization was followed both in mesocosms
301 filled with the ‘native soils’, i.e. the original corresponding microplot soil, as well as in parallel
302 filled with a constant ‘reference soil’ (the loamy sand soil from plot 1-1) across all sites. . Around
303 three months after incorporation, the percentage of ryegrass-C mineralized in the native soils
304 followed the order: loam ($63\pm 5\%$) > silt loam ($48\pm 7\%$) > loamy sand ($39\pm 7\%$) ($P<0.05$; $n=6$) (Fig.
305 4). Similarly, the percentage of ryegrass-C mineralized in the mesocosms filled with the loamy
306 sand reference soil was higher in the loam soil ($49\pm 3\%$) than in the silt loam soil ($36\pm 5\%$, $P<0.05$;
307 $n=6$) (Fig. 4). A larger part of added ryegrass-C was mineralized in the native loam and silt loam
308 soils than in the reference mesocosms buried in the corresponding plots ($P<0.01$; $n=6$). No likewise
309 statistical difference existed between native loamy sand soils and corresponding reference soils
310 (Fig. 4).

311

312

313

314

315

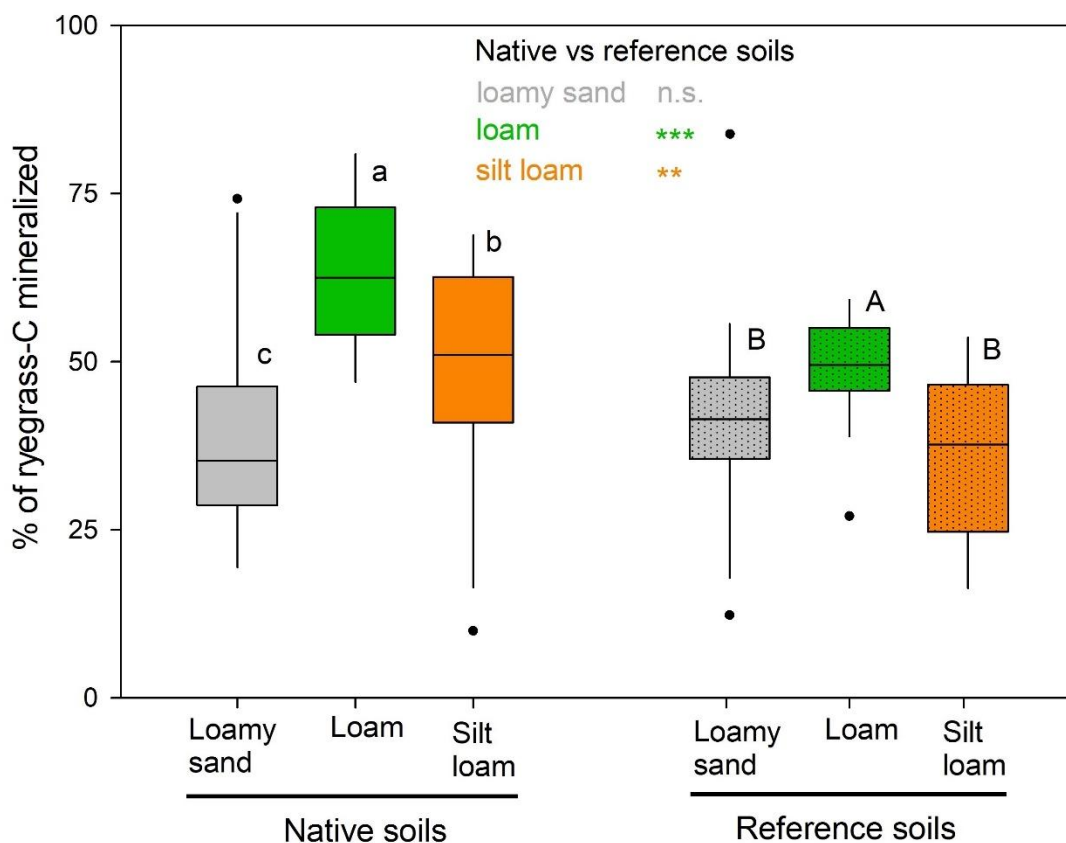
316

317

318

319

320



321

322 **Fig. 4** Percentage of added ryegrass-C mineralized three months since incorporation. Lowercase
323 and uppercase letters denote significant differences between soil texture classes for the native and
324 reference soils, respectively ($P < 0.05$). ** and *** denote significant differences ($P < 0.01$ and
325 $P < 0.001$) between native and reference soil pairs per texture class. 'n.s.' indicates that there was
326 no significant difference between both.

327

328 3.3.2 Remnant ryegrass-C

329 More undecomposed ryegrass-C (i.e. ryegrass-C $> 500 \mu\text{m}$) was left in the native loamy sand ($32 \pm 3\%$
330 of added ryegrass-C) and silt loam soils ($23 \pm 3\%$) than in the loam soils ($15 \pm 2\%$, $P < 0.05$; $n=6$)

331 (Fig. 5). In the reference soil buried in silt loam soils, a larger share of added ryegrass-C (> 500
332 μm) was left undecomposed ($37\pm 4\%$) compared to that in the loam soils ($23\pm 2\%$, $P < 0.05$; $n=6$)
333 (Fig. 5). In contrast, the remnant ryegrass-derived SOC fraction (i.e. ryegrass-C in the <500 μm
334 soil fraction) did not differ between the soil textures, neither for native soil nor reference soil
335 mesocosms. Across all 36 soil/treatment (reference or native soil) combinations, the average
336 percentage of added undecomposed ryegrass-C residing in the <500 μm fraction was $27\pm 1\%$.

337

338

339

340

341

342

343

344

345

346

347

348

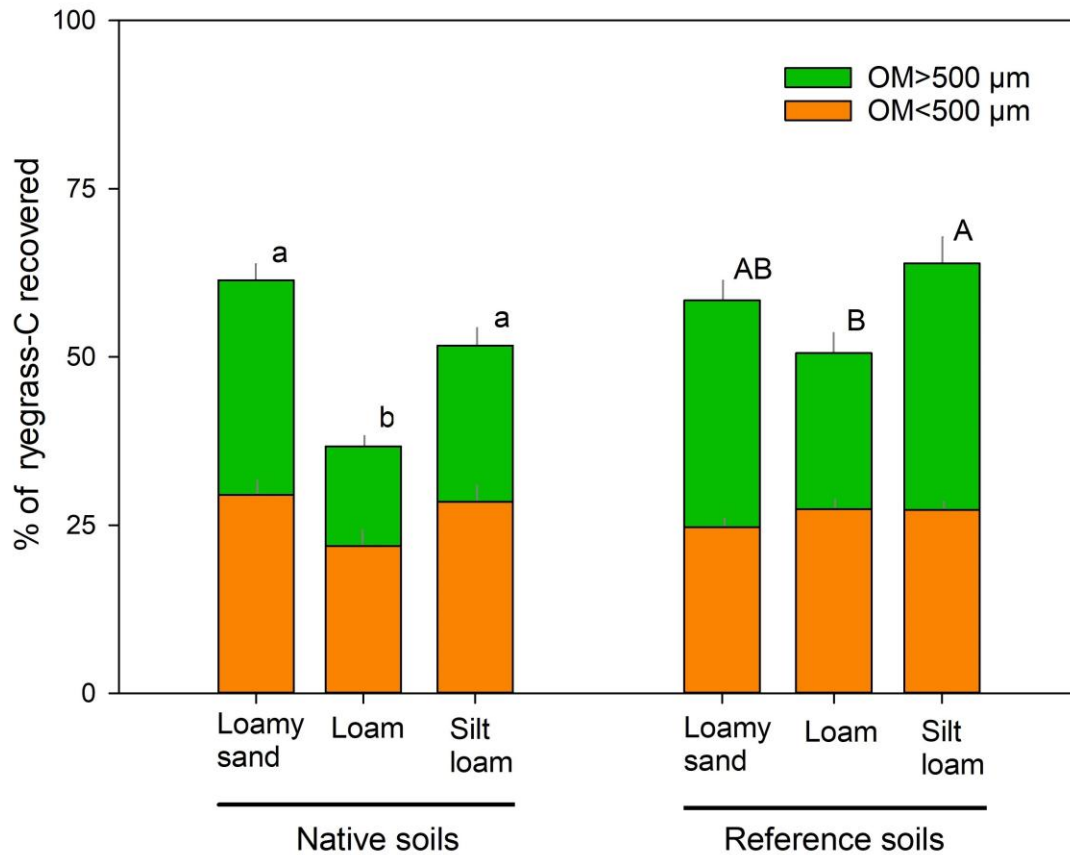
349

350

351

352

353



354

355 **Fig. 5** Percentage of added ryegrass-C remnant in the >500 μm and <500 μm soil fractions three
 356 months since incorporation. Lowercase and uppercase letters denote significant differences in
 357 remnant OM>500μm between soil textures for the native and reference soils, respectively ($P <$
 358 0.05). The percentage of remnant OM<500μm did not differ with texture.

359

360 4. Discussion

361 4.1. Overall differences in ryegrass-C mineralization between the three soil textural classes

362 Fine mineral particles (silt and clay) can protect added OM from mineralization directly by binding
 363 the OM, or by forming micro-aggregates and micro-pores within soil. This partially renders the
 364 OM inaccessible to microorganisms (Hassink, 1992; Beare et al., 1994; Krull et al., 2003).
 365 Surprisingly, the ryegrass-C mineralized in the loamy sand soils was 24% and 9% lower than in

366 the loam and silt loam soils, respectively (Fig. 4). Similarly, the percentage of ryegrass-C
367 mineralized was lower in the reference soil (loamy sand) mesocosms buried in the loam and silt
368 loam fields compared to ryegrass-C mineralization in corresponding the native soils. These results
369 contradict to the widespread expectation that OM mineralization would be generally retarded in
370 finer textured soil, owing to enhanced physicochemical protection of OM (Amato et al., 1987;
371 Hassink, 1992; Côté et al., 2000; Angst et al., 2021). To explain this discrepancy, other factors
372 known to influence soil microbial activity, such as might have co-varied with soil texture: pH,
373 soil N, SOC, soil temperature, and soil moisture content need to be considered. The pH_{KCl} was
374 statistically similar among the textural classes and limitations in available N were avoided by
375 adding a sufficient amount of mineral N to all soil mesocosms. Moreover, all soils had a similar
376 low C/N ratio (~9) and the ryegrass substrate itself had a C/N ratio of 12.8, which can be expected
377 to result in net N release. While pH and N availability affect OM mineralization (Pietri and
378 Brookes, 2008; Maenhout et al., 2018), we can assume that the observed strong dependency of
379 ryegrass-C mineralization on soil texture was not caused by differences in these parameters. Native
380 SOC content, which varied among the three textural classes, may also influence mineralization of
381 added OM (Franzluebbers et al., 1995). Overall there was a weak positive correlation between
382 SOC and the silt and clay content ($r = 0.66$; $p < 0.05$) and particularly the higher native SOC level
383 of the silt loam soils may have provided more favorable conditions for microorganisms compared
384 to the loamy sand soils and this may have masked a direct stabilizing effect of finer texture.
385 However, this explanation does not account for the higher percentage of decomposed ryegrass-C
386 in the loam soils, given that its SOC content did not differ from that of the loamy sand soils. All
387 microbial-mediated processes, including OM mineralization, are highly sensitive to soil
388 temperature (Kirschbaum, 1995; Davidson and Janssens, 2006). Coarse-textured soils absorb heat

389 faster than fine-textured soils in top 10 cm (Akter et al., 2015;). Vice-versa, soil cooling also
390 depends on soil texture. This textural control on soil temperature may in turn influence moisture
391 content. Our data showed that the soil temperature was not statistically significant between all soils
392 (Fig. 2b) and therefore variation in observed ryegrass-C mineralization could not have stemmed
393 from temperature differences between the three considered soil texture classes (Table S1). Lastly,
394 there existed a significant difference in moisture content among the three textures, suggesting a
395 potential indirect influence of soil texture on the ryegrass mineralization via mediation of soil
396 moisture, as discussed further in 4.2.

397

398 *4.2. Indirect effects of soil texture on ryegrass-C mineralization through moisture*

399 Soil moisture influences OM mineralization directly through its effect on physiological processes
400 of microorganisms and indirectly via regulating substrate and oxygen diffusion, enzyme activity
401 and osmotic stress (Moyano et al., 2013). Previous studies have shown that OM mineralization
402 may be unaffected in finer-textured soils during extended drought periods, primarily due to their
403 larger water holding capacity. In contrast, microbial activity would be inhibited in coarser-textured
404 soils (Dilustro et al., 2005; Li et al., 2020; 2022). As expected, the loamy sand soils had a lower
405 mean WFPS (37%) throughout the summer monitoring period than the loam soils (54%), which
406 approached the optimum level for aerobic heterotrophic activity (Skopp et al., 1990; Moyano et
407 al., 2013). Against our expectations, the silt loam soils also had a rather low mean WFPS (37%)
408 throughout the experimental period. The trends in ryegrass-C mineralization, both in the reference
409 and the native soils were in line with these trends in %WFPS and across all soils, the %WFPS
410 correlated positively with the percentage of added ryegrass-C decomposed. Within each soil
411 textural classes, no such relation was found between %WFPS and ryegrass-C mineralization,

412 suggesting factors other than soil texture had limited influence on soil moisture and ryegrass-C
413 mineralization variation. These combined results suggest that differences in %WFPS between the
414 considered soil texture classes determined OM mineralization. In other words, there was a clear
415 indirect control of soil texture on OM mineralization via its impact on soil moisture. This indirect
416 influence appeared to be sizable in the studied dry summer, with a doubling of OM mineralization
417 in the wettest (loam) soils than in the driest (loamy sand) plots, but we did not detect such indirect
418 impact on OM mineralization between loam and silt loam soils. Nonetheless, this outcome stresses
419 the need for accurate simulation of the soil texture-mediated topsoil moisture balance in soil C
420 models.

421 It is noteworthy that the dependency of remnant ryegrass-C on soil texture was very different for
422 the two soil fractions considered. The remaining ryegrass-C in the $<500\ \mu\text{m}$ fraction was not
423 significantly different among the three soil textures, whereas the ryegrass-C left in the $>500\ \mu\text{m}$
424 fraction, i.e. remnant added ryegrass pieces, varied with soil texture. This result contradicts the
425 view that soil texture has a limited impact on unprotected OM while it mainly regulates finer OM
426 in soil through physicochemical interactions (Plante et al., 2006). Again, the preservation of over
427 double the amount of $>500\ \mu\text{m}$ ryegrass-C in the loamy sand than in the loam soils could not be
428 explained by any direct textural effect. Rather, it again appears that mineralization of C in these
429 larger OM pieces was more sensitive to the moisture content, that co-varied with the texture, than
430 the finer ryegrass-derived-C ($<500\ \mu\text{m}$). This is likely due to the location of the ryegrass pieces in
431 macropores, which are more readily subject to desiccation than finer pores containing smaller-
432 sized OM in the loamy sand and silt loam soils. The significantly higher WFPS% in the loam soils
433 might have been sufficient to prevent desiccation of the coarse ryegrass pieces, and this would
434 explain why much less ryegrass-C was left ($15\pm 2\%$) than in the loamy sand soil ($32\pm 3\%$) (Fig. 5).

435 In contrast, ryegrass-C in the <500 μm fraction likely resided in smaller pores that remained mostly
436 moist across all three investigated textural classes. Therefore, soil texture could not have indirectly
437 controlled mineralization of this finer sized ryegrass-derived OM via its effect on the soil moisture
438 content (Fig. 5). Further experimental proof for the postulated indirect effect of soil texture on
439 large-sized OM mineralization could follow from observation of the location of OM in the soil
440 matrix relative to water-filled pores, e.g. via X-ray CT scanning of soil cores.

441 *4.3 Effects of capillary rise on topsoil moisture supply and ryegrass-C mineralization*

442 The study area experienced an unusual dry summer in 2020, with 35% less precipitation compared
443 to the corresponding period in 1992-2013. It is thus not surprising that %WFPS often dropped
444 below 40%WFPS in the loamy sand soils, while the heavier-textured loam soils remained at
445 ~55%WFPS (Gupta and Larson, 1979). However, the finer-textured silt loam fields also dried out
446 during this dry summer. To explain these contrasts in %WFPS and concurrent larger ryegrass-C
447 mineralization in the loam soils, it is relevant to compare the potential for water supply from
448 subsoil, which can form a significant supply of topsoil moisture aside from precipitation (Zipper
449 et al., 2015; Smith et al., 2017; Qiu et al., 2019). Especially in situations with shallow GWT,
450 capillary rise may serve as a crucial water supply to the topsoil in finer textured soils during
451 prolonged drought, whereas its effect is likely limited in coarse-textured soils due to the restricted
452 maximum height of capillary rise (0.2 to 1.3 m) (Hassink, 1994; Liu et al., 2014; Marchionni et
453 al., 2020). In this study, the GWT in the loamy sand soils was ~2 m or deeper during the summer
454 period (Fig. 3), making capillary feeding of the topsoil moisture highly unlikely. Except for three
455 of the loam soils and three of the silt loam plots, GWT was above 2.5 m depth during the
456 experimental period. Since the maximum height for capillary rise can be ~2 m in loam and as much
457 as 3 m in silt loam soils (Liu et al., 2014; Salim, 2016), moisture supply from groundwater was

458 thus likely to reach topsoil via capillary rise in these finer textured soils. To further explore this,
459 we converted measured soil moisture contents from 15 cm and 45 cm depths to water potentials
460 using soil layer specific fitted Van Genuchten models (Van Genuchten, 1980) and calculated water
461 potential gradients. Water potential gradients from 45 cm to 15 cm depth were small or close to
462 zero in the loamy sand soils throughout the experimental period, but they were positive in most
463 loam and silt loam soils (Fig. 6). This indicates upward water transport between these two layers,
464 suggesting groundwater was potentially a relevant source of water in the loam and silt loam
465 topsoils. However, water potential gradients and GWT depths were comparable in the loam and
466 silt loam soil, indicating that the higher topsoil %WFPS in the loam soils cannot be fully explained
467 by a substantially larger moisture supply from the groundwater than in the silt loam soils. Another
468 likely explanation for systematically wetter conditions in the loam soils seems to be their
469 antecedent wetter condition in March 2020. Other factors such as field slope or vegetation water
470 uptake, not accounted for in this study, might also have systematically influenced the initial
471 moisture levels between both textural classes (Xu and Wan, 2008; Vereecken et al., 2022), causing
472 unexplained spatial variability in OM mineralization at the landscape level. These results once
473 again reinforce the complexity of soil matrix under field conditions. Nevertheless, our analysis
474 illustrated that capillary water from shallow groundwater contributed little to topsoil moisture
475 supply in coarse-textured soil and consequently it had limited impacts on OM mineralization.
476 Future research using differences in isotopic signature (such as $\delta^{18}\text{O}$) between precipitation and
477 groundwater could shed more light on the relative contribution of both sources on topsoil water
478 supply and its further impact on OM mineralization during dry summers.

479

480

481

482

483

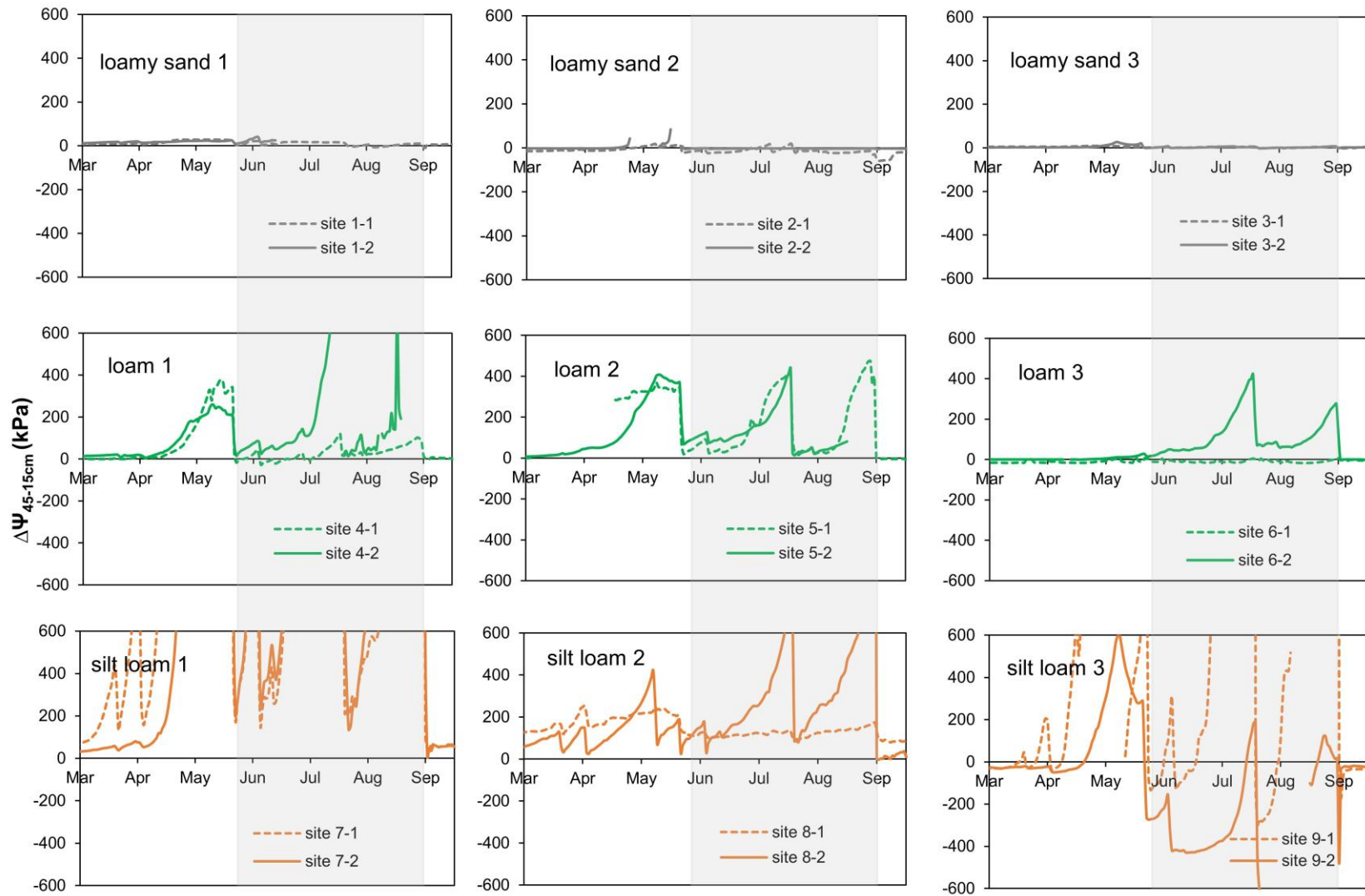
484

485

486

487

488



489
 490 **Fig. 6** Difference in soil water potential ($\Delta\Psi$) at 45 cm and 15 cm depth. The grey rectangle shade indicates the experimental period.

491 Positive values indicate more negative water potentials at 15 than at 45cm depth, i.e. conditions that would allow for upward capillary
492 transport of soil moisture.

493 4.4. Implications for SOC dynamics

494 Generally it is assumed that soil texture exerts a relevant ‘direct’ effect on OM mineralization, by
495 regulating opportunity for OM protection via organo-mineral interaction or physical occlusion.
496 However, our results demonstrate that a “direct” effect of soil texture on fresh OM mineralization
497 was limited under field conditions. This in fact corroborates several other studies (Jenkinson and
498 Ayanaba, 1977; Sugihara et al., 2012), including our previous observation (Li et al., 2022) that
499 added maize shoots mineralization was not impacted by soil texture in the first months after field
500 incorporation in autumn. These results are in contrast with the direct textural factors for
501 decomposition rates of labile-C pools that are usually included in the algorithms of most soil C
502 models. For instance, the Roth-C model includes clay content as a factor to estimate the ratio
503 between CO₂ produced and the sum of humified organic matter and microbial biomass formed
504 during the decomposition of decomposable plant material (DPM) and resistant plant material
505 (RPM) (Coleman and Jenkinson, 1996). The ryegrass residues studied here would be partitioned
506 40% in the RPM pool and 60% in the DPM pool. The DPM pool has a turnover time of a few
507 months, corresponding to the observed percentage of ryegrass-C mineralization and the time scale
508 of this field experiment. Our findings suggest the Roth-C model to be overly sensitive to the factor
509 soil texture for simulation of the decomposition of this 60% DPM pool. The DNDC model (Li et
510 al., 1992) also includes clay as a controller of the OM decomposition rate, with factors 1.00-1.67
511 and 0.35-1.00 for coarse-textured and fine-textured soils, respectively. This textural decomposition
512 rate modification applies to all of DNDC’s OM pools, i.e., plant residues, microbial biomass,
513 humads and humus. Again, our results challenge DNDC’s algorithms for simulating the
514 decomposition of the plant residue OC-pool as a function of soil texture.

515 Over the past years, Europe and many other regions in the world have experienced severe summer
516 droughts and current climate models predict more frequent summer droughts under future climate
517 change scenarios (Vicente-Serrano et al., 2014; Hanel et al., 2018). Summer drought not only
518 imposes a severe threat on the agricultural sector but also reduces litter-derived C mineralization
519 (Joos et al., 2010). Our results imply that soil texture-mediated moisture played a non-negligible
520 role on OM mineralization during dry summers, even in a maritime climate with an even
521 distribution of precipitation across the year and an overall precipitation surplus of 300 mm.
522 However, the indirect impacts of soil texture on OM mineralization through mediation of moisture
523 appear insufficiently accounted for by current soil C models. For instance, water inputs to topsoil
524 from capillary rise are not simulated by most models, including DNDC and Roth-C. We found that
525 upward capillary flow was rather limited in sustaining topsoil water input in loamy sand soils when
526 GWT was deeper than 1.5 m. However, water input from subsoil to topsoil was suggested to occur
527 in the finer textured soils, potentially forming an important component in the topsoil water balance
528 during prolonged summer droughts. Therefore, in future climate with more incidence of prolonged
529 dry periods, it will become even more pertinent to properly simulate soil water balances for
530 simulating SOC dynamics precisely, as moisture availability becomes the main controller of OM
531 mineralization.

532 **5. Conclusion**

533 We monitored OM mineralization in nine agricultural fields during a dry summer and
534 demonstrated that direct effects of soil texture on OM mineralization played a minor role in the
535 short term. This suggests that textural-modifiers of C mineralization in C models might be overly
536 sensitive for the considered labile C pools. Instead, our analysis suggests that soil texture can
537 control fresh OM mineralization indirectly through moisture in the short term. The mineralization

538 of OM in loam soils was higher than in loamy sand and silt loam soils due to the higher moisture
539 content (54%WFPS). This indirect textural effect was significant for OM in the larger soil size
540 fraction (here added ryegrass >500 μm), but not for OM in the finer soil fraction (<500 μm). We
541 hypothesize this contrasting sensitivity to texture to be related with more frequent drying out of
542 large soil pores during droughts, while finer pores remain sufficiently moist for microbial activity
543 to proceed. Capillary rise from subsoil was indicated to have contributed to topsoil moisture in
544 loam and silt loam but not in the loamy sand fields in the study area. In this way, soil texture could
545 have additionally indirectly controlled OM mineralization. This indirect textural control during
546 drought obviously only occurs when soil texture predominantly determines soil moisture, and with
547 many more here unaccounted for components of the soil water balance, it is perhaps unsurprising
548 that soil texture only poorly explained the differences in soil moisture and OM mineralization
549 between the loam and silt loam pairs. Our findings call for a proper simulation of the soil water
550 balance of entire soil profiles if soil carbon models are to be used to simulate SOC dynamics under
551 future climate scenarios.

552 **Acknowledgements**

553 This study was funded by Research Foundation - Flanders (FWO:1523719N and G066020N).
554 Haichao Li was supported by the China Scholarship Council (CSC). We would like to thank
555 Mathieu Schatteman and Ezeakunne Ugochukwu Victor for the field and laboratory work.
556 Moreover, we are grateful to the farmer Patric Buggenhout for providing access to his silt loam
557 fields.

558 **References**

559 Akter, M., Miah, M. A., Hassan, M. M., Mobin, M. N., Baten, M. A., 2015. Textural influence on
560 surface and subsurface soil temperatures under various conditions. *Journal of Environmental*
561 *Science and Natural Resources*, 8(2), 147–151.

562 Amato, M., Ladd, J. N., Ellington, A., Ford, G., Mahoney, J. E., Taylor, A. C., Walscott, D., 1987.
563 Decomposition of plant material in Australian soils. IV. Decomposition *in situ* of ¹⁴C labeled and
564 ¹⁵N labeled legume and wheat materials in a range of southern Australian soils. *Soil Research*,
565 25(1), 95–105.

566 Angst, G., Pokorný, J., Mueller, C. W., Prater, I., Preusser, S., Kandeler, E., Meador T., Straková
567 P., Hájek T., van Buiten G., Angst, Š., 2021. Soil texture affects the coupling of litter
568 decomposition and soil organic matter formation. *Soil Biology and Biochemistry*, 159, 108302.

569 Balesdent, J., Balabane, M., 1996. Major contribution of roots to soil carbon storage inferred from
570 maize cultivated soils. *Soil Biology and Biochemistry*, 28(9), 1261–1263.

571 Barré, P., Angers, D. A., Basile-Doelsch, I., Bispo, A., Cécillon, L., Chenu, C., Chevallier T.,
572 Derrien D., Eglin T. K., Pellerin, S., 2017. Ideas and perspectives: Can we use the soil carbon
573 saturation deficit to quantitatively assess the soil carbon storage potential, or should we explore
574 other strategies?. *Biogeosciences Discussions*, 1–12.

575 Beare, M.H., Hendrix, P.F., Cabrera, M.L., Coleman, D.C., 1994. Aggregate-protected and
576 unprotected organic matter pools in conventional-and no-tillage soils. *Soil Science Society of*
577 *America Journal* 58 (3), 787–795.

578 Blanco-Moure, N., Gracia, R., Bielsa, A. C., López, M. V., 2016. Soil organic matter fractions as
579 affected by tillage and soil texture under semiarid Mediterranean conditions. *Soil and Tillage*
580 *Research*, 155, 381–389.

581 Burke, I. C., Yonker, C. M., Parton, W. J., Cole, C. V., Flach, K., Schimel, D. S., 1989. Texture,
582 climate, and cultivation effects on soil organic matter content in US grassland soils. *Soil Science*
583 *Society of America Journal*, 53(3), 800–805.

584 Coleman, K., Jenkinson, D. S., 1996. RothC-26.3-A Model for the turnover of carbon in soil, In
585 *Evaluation of soil organic matter models*. Springer, Berlin, Heidelberg, pp. 237–246.

586 Côté, L., Brown, S., Paré, D., Fyles, J., Bauhus, J., 2000. Dynamics of carbon and nitrogen
587 mineralization in relation to stand type, stand age and soil texture in the boreal mixedwood. *Soil*
588 *Biology and Biochemistry*. 32, 1079–1090.

589 Davidson, E. A., Janssens, I. A., 2006. Temperature sensitivity of soil carbon decomposition and
590 feedbacks to climate change. *Nature*, 440(7081), 165–173.

591 Dilustro, J. J., Collins, B., Duncan, L., Crawford, C., 2005. Moisture and soil texture effects on
592 soil CO₂ efflux components in southeastern mixed pine forests. *Forest Ecology and Management*,
593 204(1), 87–97.

594 Fan, Y., Li, H., Miguez-Macho, G., 2013. Global patterns of groundwater table depth. *Science*,
595 339(6122), 940–943.

596 Feller, C., Chenu, C., 2012. Les interactions bio-organo-argileuses et la stabilisation du carbone
597 dans les sols. *Etude et Gestion des Sols*, 19, 235–248 (in French).

598 Franzluebbers, A. J., 1999. Microbial activity in response to water-filled pore space of variably
599 eroded southern Piedmont soils. *Applied Soil Ecology*, 11(1), 91–101.

600 Franzluebbbers, A. J., Hons, F. M., Zuberer, D. A., 1995. Soil organic carbon, microbial biomass,
601 and mineralizable carbon and nitrogen in sorghum. *Soil Science Society of America Journal*, 59(2),
602 460–466.

603 Geroy, I. J., Gribb, M. M., Marshall, H. P., Chandler, D. G., Benner, S. G., McNamara, J. P., 2011.
604 Aspect influences on soil water retention and storage. *Hydrological Processes*, 25(25), 3836–3842.

605 Gupta, S., Larson, W. E., 1979. Estimating soil water retention characteristics from particle size
606 distribution, organic matter percent, and bulk density. *Water resources research*, 15(6), 1633–1635.

607 Hanel, M., Rakovec, O., Markonis, Y., Máca, P., Samaniego, L., Kyselý, J., Kumar, R., 2018.
608 Revisiting the recent European droughts from a long-term perspective. *Scientific Reports*, 8(1), 1–
609 11.

610 Hassink, J., 1992. Effects of soil texture and structure on carbon and nitrogen mineralization in
611 grassland soils. *Biology and Fertility of Soils*, 14(2), 126–134.

612 Hassink, J., 1994. Effects of soil texture and grassland management on soil organic C and N and
613 rates of C and N mineralization. *Soil Biology and Biochemistry*, 26(9), 1221–1231.

614 Jenkinson, D. S., 1990. The turnover of organic carbon and nitrogen in soil. *Philosophical*
615 *Transactions of the Royal Society of London. Series B: Biological Sciences*, 329(1255), 361–368.

616 Jenkinson, D. S., Ayanaba, A., 1977. Decomposition of carbon-14 labeled plant material under
617 tropical conditions. *Soil Science Society of America Journal*, 41(5), 912–915.

618 Joos, O., Hagedorn, F., Heim, A., Gilgen, A. K., Schmidt, M. W., Siegwolf, R. T. W., Buchmann,
619 N., 2010. Summer drought reduces total and litter-derived soil CO₂ effluxes in temperate
620 grassland—clues from a ¹³C litter addition experiment. *Biogeosciences*, 7(3), 1031–1041.

621 Kirschbaum, M. U., 1995. The temperature dependence of soil organic matter decomposition, and
622 the effect of global warming on soil organic C storage. *Soil Biology and Biochemistry*, 27(6), 753–
623 760.

624 Koenig, W. D., Liebhold, A. M., 2016. Temporally increasing spatial synchrony of North
625 American temperature and bird populations. *Nature Climate Change*, 6(6), 614-617.

626 Krull, E.S., Baldock, J.A., Skjemstad, J.O., 2003. Importance of mechanisms and processes of the
627 stabilisation of soil organic matter for modelling carbon turnover. *Functional Plant Biology* 30 (2),
628 207–222.

629 Li, C., Frohking, S., Frohking, T. A., 1992. A model of nitrous oxide evolution from soil driven by
630 rainfall events: 1. Model structure and sensitivity. *Journal of Geophysical Research: Atmospheres*,
631 97(D9), 9759–9776.

632 Li, H., Van den Bulcke, J., Mendaza, O., Deroo, H., Haesaert G., Dewitte K., De Neve S., Sleutel
633 S., 2021. Soil texture controls added organic matter mineralization by regulating soil moisture—
634 evidence from a field experiment in a maritime climate. *Geoderma*, 410, 115690.

635 Li, H., Van den Bulcke, J., Wang, X., Gebremikael, M. T., Hagan, J., De Neve, S., Sleutel, S.,
636 2020. Soil texture strongly controls exogenous organic matter mineralization indirectly via
637 moisture upon progressive drying—Evidence from incubation experiments. *Soil Biology and*
638 *Biochemistry*, 151, 108051.

639 Liu, Q., Yasufuku, N., Miao, J., Ren, J., 2014. An approach for quick estimation of maximum
640 height of capillary rise. *Soils and Foundations*, 54(6), 1241–1245.

641 Maenhout, P., Van den Bulcke, J., Van Hoorebeke, L., Cnudde, V., De Neve, S., Sleutel, S., 2018.
642 Nitrogen limitations on microbial degradation of plant substrates are controlled by soil structure
643 and moisture content. *Frontiers in microbiology*, 9, 1433.

644 Marchionni, V., Daly, E., Manoli, G., Tapper, N. J., Walker, J. P., Fatichi, S., 2020. Groundwater
645 buffers drought effects and climate variability in urban reserves. *Water Resources Research*, 56(5),
646 e2019WR026192.

647 Moyano, F. E., Manzoni, S., Chenu, C., 2013. Responses of soil heterotrophic respiration to
648 moisture availability: An exploration of processes and models. *Soil Biology and Biochemistry*, 59,
649 72–85.

650 Muller, T., Hoper, H., 2004. Soil organic matter turnover as a function of the soil clay content:
651 consequences for model applications. *Soil Biology and Biochemistry*, 36, 877–888.

652 Parton, W. J., Schimel, D. S., Cole, C. V., Ojima, D. S., 1987. Analysis of factors controlling soil
653 organic matter levels in Great Plains grasslands. *Soil Science Society of America Journal*, 51(5),
654 1173–1179.

655 Pietri, J. A., Brookes, P. C., 2008. Relationships between soil pH and microbial properties in a UK
656 arable soil. *Soil Biology and Biochemistry*, 40(7), 1856–1861.

657 Plante, A. F., Conant, R. T., Stewart, C. E., Paustian, K., Six, J., 2006. Impact of soil texture on
658 the distribution of soil organic matter in physical and chemical fractions. *Soil Science Society of*
659 *America Journal*, 70(1), 287–296.

660 Poll, C., Marhan, S., Back, F., Niklaus, P. A., Kandeler, E., 2013. Field-scale manipulation of soil
661 temperature and precipitation change soil CO₂ flux in a temperate agricultural ecosystem.
662 *Agriculture, Ecosystems & Environment*, 165, 88–97.

663 Qiu, J., Zipper, S. C., Motew, M., Booth, E. G., Kucharik, C. J., Loheide, S. P., 2019. Nonlinear
664 groundwater influence on biophysical indicators of ecosystem services. *Nature Sustainability*, 2(6),
665 475–483.

666 Ruel, J. J., Ayres, M. P., 1999. Jensen's inequality predicts effects of environmental variation.
667 *Trends in Ecology & Evolution*, 14(9), 361–366.

668 Salim, R. L., 2016. Extent of Capillary Rise in Sands and Silts. Master's Thesis, Western Michigan
669 University, USA.

670 Scott, N. A., Cole, C. V., Elliott, E. T., Huffman, S. A., 1996. Soil textural control on
671 decomposition and soil organic matter dynamics. *Soil Science Society of America Journal*, 60(4),
672 1102–1109.

673 Skopp, J., Jawson, M. D., Doran, J. W., 1990. Steady-state aerobic microbial activity as a function
674 of soil water content. *Soil Science Society of America Journal*, 54(6), 1619–1625.

675 Smith, A. P., Bond-Lamberty, B., Benschoter, B. W., Tfaily, M. M., Hinkle, C. R., Liu, C., Bailey,
676 V. L., 2017. Shifts in pore connectivity from precipitation versus groundwater rewetting increases
677 soil carbon loss after drought. *Nature Communications*, 8(1), 1–11.

678 Sugihara, S., Funakawa, S., Kilasara, M., Kosaki, T., 2012. Effects of land management on CO₂
679 flux and soil C stock in two Tanzanian croplands with contrasting soil texture. *Soil Biology and*
680 *Biochemistry*, 46, 1–9.

681 Thomsen, I. K., Schjønning, P., Jensen, B., Kristensen, K., Christensen, B. T., 1999. Turnover of
682 organic matter in differently textured soils: II. Microbial activity as influenced by soil water
683 regimes. *Geoderma*, 89(3–4), 199–218.

684 Van Genuchten, M.T., 1980. A closed-form equation for predicting the hydraulic conductivity of
685 unsaturated soils. *Soil Science Society of America Journal*. 44 (5), 892–898.

686 Van Genuchten, M. V., Leij, F. J., Yates, S. R., 1991. The RETC code for quantifying the hydraulic
687 functions of unsaturated soils.

688 Van Veen, J. A., Ladd, J. N., Amato, M., 1985. Turnover of carbon and nitrogen through the
689 microbial biomass in a sandy loam and a clay soil incubated with [¹⁴C(U)]glucose and
690 [¹⁵N](NH₄)₂SO₄ under different moisture regimes. *Soil Biology and Biochemistry*, 17(6), 747–756.

691 Vereecken, H., Amelung, W., Bauke, S. L., Boga, H., Brüggemann, N., Montzka, C.,
692 Vanderborght J., Bechtold M., Blöschl G., Carminati A., Javaux M., Konings A. G., Kusche J.,
693 Neuweiler I., Or D., Steele-Dunne S., Verhoef A., Young M., Zhang, Y., 2022. Soil hydrology in
694 the Earth system. *Nature Reviews Earth & Environment*, 1–15.

695 Vicente-Serrano, S. M., Lopez-Moreno, J. I., Beguería, S., Lorenzo-Lacruz, J., Sanchez-Lorenzo,
696 A., García-Ruiz, J. M., Azorin-Molina C., Morán-Tejeda E., Revuelto J., Trigo R., Coelho F.,
697 Espejo, F., 2014. Evidence of increasing drought severity caused by temperature rise in southern
698 Europe. *Environmental Research Letters*, 9(4), 044001.

699 Wang, W. J., Dalal, R. C., Moody, P. W., Smith, C. J., 2003. Relationships of soil respiration to
700 microbial biomass, substrate availability and clay content. *Soil Biology and Biochemistry*, 35(2),
701 273–284.

702 Xu, W., Wan, S., 2008. Water-and plant-mediated responses of soil respiration to topography, fire,
703 and nitrogen fertilization in a semiarid grassland in northern China. *Soil Biology and Biochemistry*,
704 40(3), 679–687.

705 Zhang, Z. S., Dong, X. J., Xu, B. X., Chen, Y. L., Zhao, Y., Gao, Y. H., Hu Y.G., Huang, L., 2015.
706 Soil respiration sensitivities to water and temperature in a revegetated desert. *Journal of*
707 *Geophysical Research: Biogeosciences*, 120(4), 773-787.

708 Zipper, S. C., Soylu, M. E., Booth, E. G., Loheide, S. P., 2015. Untangling the effects of shallow
709 groundwater and soil texture as drivers of subfield–scale yield variability. *Water Resources*
710 *Research*, 51(8), 6338–6358.

711 Zuur, A., Ieno, E. N., Walker, N., Saveliev, A. A., Smith, G. M., 2009. *Mixed effects models and*
712 *extensions in ecology with R*. Springer Science & Business Media, New York, USA.